



## Li intercalation in aluminosilicate fracture fills at Glen Rosa targets, Gale crater, Mars

Elisabeth Losa-Adams<sup>1</sup>, Alberto G. Fairén<sup>1,2</sup>, and Luis Gago-Duport<sup>3</sup>

<sup>1</sup>Centro de Astrobiología (CAB), CSIC-INTA, Carretera de Ajalvir km 4, 28850 Torrejón de Ardoz, Madrid, Spain

<sup>2</sup>Department of Astronomy, Cornell University, Ithaca, 14853 NY, USA

<sup>3</sup>Departamento de Geociencias Marinas, Universidade de Vigo, Lagoas-Marcosende, Vigo, Spain

The ChemCam instrument onboard the Mars Science Laboratory has detected elevated values of Lithium (Li) in Si-Al-filled fractures throughout the sedimentary layers of the crater Gale. Previous studies have associated the abundance of Li in calcium sulphate veins with the degree of dehydration of diagenetic fluids [1], but the final reservoir of Li in the last evaporation stage remains unknown. Since elevated Li abundance in secondary minerals provides insights into the extension and intensity of Martian aqueous processes [2, 3], we evaluated the geochemical significance and possible mechanisms of Li incorporation into their minerals.

The Li concentration of the rock as a whole along the stratigraphic sequence (Figure 1) shows average values similar to Earth's Middle Ocean Ridge basalts (MORB ~ 6,5 ppm) [4]. The variations in Li concentration with respect to the MORB protolith exhibit a range of  $\pm 6,5$  ppm at the majority of observation points, although there are two noteworthy exceptions. The first deviation corresponds to the Bradbury group at the crater base, where the observed Li abundance deviates by up to 120 ppm. This pattern follows a decreasing trend between members, with the Li content stabilising at values closer to MORB. The second deviation corresponds to the Glasgow member, which shows a high Li abundance in fracture-fill sediment, with values ranging from 45 to 125 ppm, with an average of 72 ppm (Figure 2). In this latter case, Li is explicitly associated with Silica-Alumina veins that cut through the fractured basalt mudstone and separate areas of veins rich in Mn/Fe minerals. Preliminary calculations based on the composition of  $\text{Al}_2\text{O}_3$  and  $\text{SiO}_2$  oxides indicate that the stoichiometry of double Al-silicates such as kaolinite or halloysite alone does not fit the observed composition of the veins. This suggests that a non-stoichiometric mixture of amorphous silica together with various aluminosilicates capable of incorporating Li, K and Mg into their structure forms the observed veins.

Here, we analyse the incorporation of Li into amorphous or partially crystallised materials derived from circulating silica-aluminium-rich solutions of basaltic weathering. These solutions have the potential to precipitate both crystalline aluminosilicates with structural Li and Al-Si hydroxide gels, which are capable of intercalating Li into their amorphous network through reverse weathering. We included in the database the possible Al-Si phases formed in the final stages of Li evaporation brines, to determine their supersaturation states. We used the LiMars code, a set of scripts based on PHREEQC software [5], which allows the geochemical modelling of Li dissolution processes from primary minerals and the kinetic precipitation of crystalline and amorphous aluminosilicate phases. The incorporation of Li into these secondary phases is an adsorption or ion exchange mechanism.

The geochemical scenario involves two solutions with opposing pH values, mixing by diffusion in an evaporative context. Depending on the pH conditions, the volcanic glass may undergo alteration into a variety of mineral assemblages. This may occur under alkaline conditions, where it may transform into Fe and Mn oxides, or during evolution to more acidic conditions, where it may evolve into hydrated volcanic glass, amorphous silica, kaolin minerals or Li-bearing Al-Si minerals. Experiments conducted with Al-Si gels formed in brines [6] showed that the highest adsorption capacity is observed at pH values of 7 - 8, which is close to the zero-loading point, and the adsorption capacity decreases at both alkaline and acidic values. This pH-dependent behaviour indicated that the neutral medium, where amorphous gels and clays precipitate, is the most favourable for Li adsorption. We hypothesise that the geochemical significance of these Al-Si veins in the Glasgow member could represent the latest stages of the evolution towards equilibrium of diagenetic fluids in Gale.

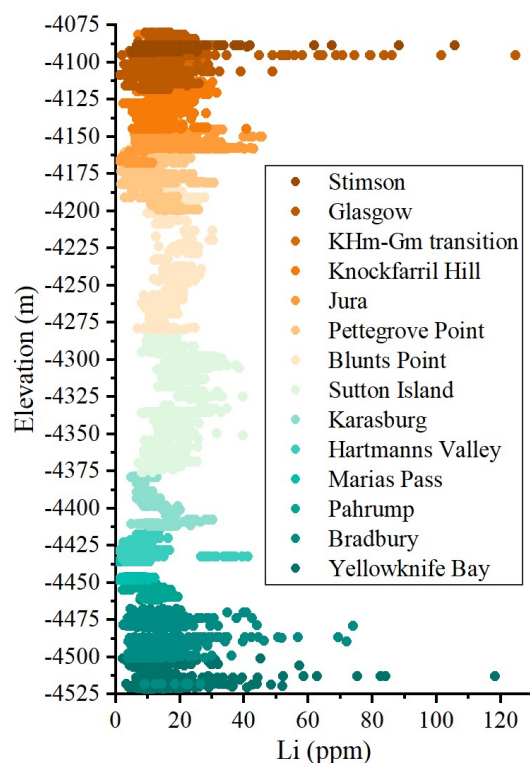


**Figure 1.** Individual ChemCam observation points plotted against elevation relative to the Martian datum for Li (ppm). The colour indicates the stratigraphic member where the points were collected. All observation points with a total sum of oxides less than 90 wt.% and those located more than 3.5 m from the ChemCam instrument were discarded. Data from Planetary Data System (PDS) Geoscience Node [7].

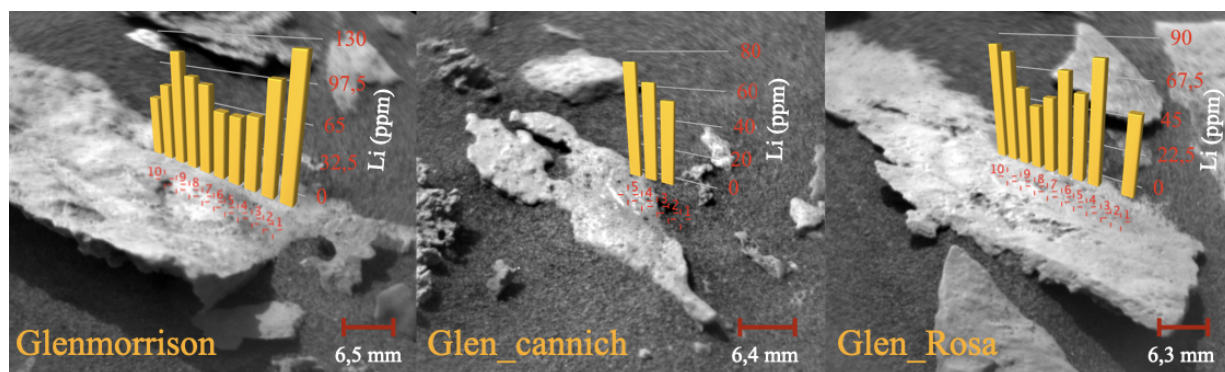


**Figure 2.** High-resolution Remote Micro-Imager (RMI) context picture of the chemical analyses performed by LIBS. Targets: Glenmorrison, Glen\_cannich and Glen\_Rosa. Data from PDS Geosciences Node [7, 8].

### **Acknowledgements**

This research has been funded by the European Research Council CoG 818602.

### **References**

- [1] Das, D. et al., 2020. *Journal of Geophysical Research: Planets*, 125(8), e2019JE006301.
- [2] Fairén, A. G. et al., 2015. *Geochemistry, Geophysics, Geosystems*, 16(4), 1172-1197.
- [3] von Strandmann, P. A. P. et al., 2020. *Elements: An International Magazine of Mineralogy, Geochemistry, and Petrology*, 16(4), 253-258.
- [4] Gale, A. et al., 2013. *Geochemistry, Geophysics, Geosystems*, 14(3), 489-518.
- [5] Parkhurst, D. L., and Appelo, C. A. J., 2013. *U.S. Geological Survey Techniques and Methods*, 6 (A43), 497.
- [6] Zhong, J. et al., 2020. *J. Colloid. Interf. Sci.* 572, 107–113.
- [7] Wiens, R. 2021c. MSL Mars ChemCam libs spectra 4/5 RDR V1.0 [Dataset]. NASA Planetary Data System.
- [8] Wiens, R. 2021d. MSL Mars ChemCam remote micro-imager camera 5 RDR V1.0 [Dataset]. NASA Planetary Data System.